Discovery of Mira variable stars in the metal-poor Sextans dwarf spheroidal galaxy

Sakamoto, Tsuyoshi[1]

sakamoto@spaceguard.or.jp

Matsunaga, Noriyuki[2,3]

Hasegawa, Takashi[4]

and

Nakada, Yoshikazu[2]

Received _____; accepted _____

Not to appear in Nonlearned J., 45.

[1]Japan Spaceguard Association, 1716-3, Ookura, Bisei, Ibara, Okayama 714-1411, Japan

[2]Kiso Observatory, Institute of Astronomy, School of Science, The University of Tokyo, 10762-30, Mitake, Kiso-machi, Kiso-gun, Nagano 397-0101, Japan

[3]Department of Astronomy, The University of Tokyo, 7-3-1 Hongo, Bunkyo-ku, Tokyo 113-0033, Japan

[4]Gunma Astronomical Observatory, 6860-86, Nakayama, Takayama, Agatsuma, Gunma 377-0702, Japan

ABSTRACT

We report the discovery of two Mira variable stars (Miras) toward the Sextans dwarf spheroidal (dSph) galaxy. We performed optical long-term monitoring observations for two red stars in the Sextans dSph. The light curves of both stars in the $I_{\rm c}$ band show large-amplitude (3.7 and 0.9 mag) and long-period (326 ± 15 and 122 ± 5 days) variations, suggesting that they are Miras. We combine our own infrared data with previously published data to estimate the mean infrared magnitudes. The distances obtained from the period-luminosity relation of the Miras ($75.3^{+12.8}_{-10.9}$ and $79.8^{+11.5}_{-9.9}$ kpc , respectively), together with the radial velocities available, support memberships of the Sextans dSph (90.0 ± 10.0 kpc). These are the first Miras found in a stellar system with a metallicity as low as [Fe/H] ~ -1.9, than any other known system with Miras.

Subject headings: Galaxy: halo — Galaxies: dwarf — stars: AGB and post-AGB

1. Introduction

Miras are pulsating stars with initial masses between 0.8 and 8 solar masses in the Asymptotic Giant Branch (AGB) phase, and eject material via stellar winds into the interstellar medium (e.g., Habing 1996). The ejected material contain chemical elements that have been dredged up from the interior (e.g., carbon and s-process elements). A large amount of dust forms in the ejecta of the Miras, and then such dust grains regulate the cooling of the interstellar medium and the fragmentation of collapsing molecular clouds into stars. Thus, Miras play an important role in providing the heavy elements and dust grains from the early Universe to the present day.

The lack of appropriate theoretical models of Miras currently prevents us from determining their fundamental properties, such as metallicities, based on observational data for Miras. Therefore, Miras in stellar systems with known metallicity and/or age distribution can be important tracers to study the evolution of Miras and their impacts on chemical enrichment. For example, most of the Galactic globular clusters are old stellar systems with a single metallicity or a narrow metallicity distribution, offering an important sample of low-mass and metal-poor Miras (Frogel & Whitelock 1998; Feast et al. 2002). We note that Miras are found only in the clusters with [Fe/H] > -1. Another interesting sample is low- to intermediate-mass Miras found in the Magellanic Clouds. A formidable amount of literature exists on those objects (e.g. Ita et al. 2004ab; Fraser et al. 2008; Soszyński et al. 2009; Groenewegen et al. 2009).

Galactic dSphs provide us with a sample of even lower metallicity objects than the globular clusters. It is known that the fainter galaxy tends to have the lower mean metallicity (Norris et al. 2010). Therefore, the faint dSphs are excellent places to study metal-poor Miras if any Mira is found. Recent monitoring surveys in Galactic dSphs have discovered several Miras (Fornax dSph, Whitelock et al. 2009; Leo I dSph, Menzies et

al. 2010; Sagittarius dSph, Lagadec et al. 2009; Sculptor dSph, Menzies et al. 2011). Among the dSphs with previously known Miras, the Sculptor dSph is the most metal deficient one, which has the metallicity distribution with a peak at [Fe/H] = −1.56 and a dispersion of 0.48 (Kirby et al. 2009). Sloan et al. (2009) reported the evidence of circumstellar dust around one of the Miras in the Sculptor dSph (Menzies et al. 2011), based on the *Spitzer Space Telescope* spectroscopy. This suggests that AGB stars in low-metallicity environments can make a significant contribution to dust formation in the early Universe.

Our target galaxy, the Sextans dSph, shows a metallicity distribution with a peak at [Fe/H] = −1.9 and is one of the most metal-poor dSphs in the Galaxy (Battaglia et al. 2011). So far, two monitoring surveys have been conducted for the center of this galaxy, revealing dozens of short-period variable stars (Mateo et al. 1995; Lee et al. 2003). No Mira has been found previously.In this paper, we report the discovery of two Miras toward the Sextans dSph. In Section 2, we describe optical and infrared photometric observations, and discuss their membership to the Sextans dSph. In Section 3, we discuss the chemical properties and their impacts.

2. Observations and Results

2.1. Our targets

In order to explore Miras in the Sextans dSph, we selected two target stars from the photometric catalogs presently available. These are listed in Table 1. The first target #1, SDSS J101525.93−020431.8, was selected using the color criteria, $J-H > 0.7$, $H-K_{\rm s} > 0.3$ on the 2MASS catalog (Skrutskie et al. 2006) and $g-r > 0.8$, $r-i > 0.3$ on the SDSS catalog (Adelman-McCarthy et al. 2008). These criteria are also used for our monitoring survey of Miras in the Galactic halo (Sakamoto et al., in preparation). The target #1 is

carbon-rich, showing a spectrum with the strong CN absorption band at 7900Å (Mauron et al. 2004; Cruz et al. 2007). The second target #2, SDSS J101234.29−013440.8, was later added because of its variation detected in QUEST1 (QUasar Equatorial Survey Team, Phase 1) variability survey (Rengstorf et al. 2009). The R-band light curve of #2 over 2 years in the QUEST1 showed a variation with a large amplitude ($\Delta R \geq 1.2$ mag) and a long period (over 100 days), although their time sampling was not good enough to estimate the period. The target #2 is oxygen-rich, showing a spectrum with clear TiO molecular absorption lines (Suntzeff et al. 1993).

2.2. I_c-band photometry

We conducted photometric monitoring observations of the two selected targets in the direction of the Sextans using the 2KCCD camera attached to the 105-cm f/3.0 Schmidt telescope at Kiso Observatory (Itoh et al. 2001).

The observations started in December 2008 and February 2010 for the targets #1 and #2, respectively, and were repeated until February 2012. Time series I_c-band images were obtained.The data were reduced following standard procedures with IRAF, including bias subtraction (both the level of the overscan region in each image and the bias pattern taken on each night) and the flat-field correction with I_c-band dome-flat images. Instrumental magnitudes of the targets and comparison stars were measured with aperture photometry using the IRAF/APPHOT package. The comparison stars were selected from the SDSS database (Adelman-McCarthy et al. 2008), and their I_c magnitudes were calculated by using the transformation of Jordi et al. (2006),

$$I_c = i' + (-0.386 \pm 0.004)(i' - z') - (0.397 \pm 0.001). \quad (1)$$

Using these I_c magnitudes for calibrating the magnitude scale, we obtained the magnitudes

of our target stars as listed in Tables 2 and 3.

Fig. 1 plots the I_c variations against the Modified Julian Date (MJD). Both stars show the long-period and large-amplitude variation characteristic of either Miras or semi-regular variables. The peak-to-valley amplitudes (ΔI_c) are 3.72 mag for the target #1 and 0.94 mag for the target #2. Miras are generally considered to have the I_c amplitude greater than 0.9-1.0 mag (Ita et al. 2004ab; Matsunaga et al. 2005). The target #1 is clearly a Mira, whereas the target #2 falls between Miras and semi-regulars.

The light curve of the target #1 shows a clear modulation over the entire observation run indicating a long-term variation which is often observed for carbon-rich Miras (Whitelock et al. 2003). We subtract this long-term trend which is fitted by a sine curve with a period of 1500 days. The residual light curve shows a regular periodic variation as expected. Then, we applied the Phase Dispersion Minimization (PDM, Stellingwerf 1978) to the residual curve to obtain a period 326 days as the best estimate. It should be noted that due to the insufficient coverage of the light curve, especially around the expected minima, we cannot exclude the possibility of the star having a period roughly half of the 326 days based only on our I_c band data. Nevertheless, the shorter period is unlikely, considering that the star is so red, $(H - K_{\rm s}) \gtrsim 1.0$, and all of such red LMC Miras in Ita et al. (2004) have periods of 300−500 days. We examined various assumptions on the long-term trend (e.g., sine curves with different periods and/or amplitudes), and the estimated period stays within 15 days from the above value. Thus, the period of #1 is estimated to be 326 ± 15 days. In contrast, the light curve of the target #2 appears to show no long-term trend, and the period of 122 days is obtained with the PDM. Sine curves with periods of 117−127 days seems consistent with the photometric data. Thus, the periods of #2 is estimated to be 122 ± 5 days.

2.3. Near-infrared photometry

For the target #1, we obtained near infrared images in the J, H, and $K_{\rm s}$-bands using the IRSF 1.4-m telescope at South African Astronomical Observatory (Nagayama et al. 2003). Our near-infrared observations were carried out on June 14, 2011 and April 28, 2012, and the magnitudes of the target were calibrated based on 2MASS magnitudes of the neighboring stars. In addition, the near-infrared magnitudes for our targets were collected from a few large-scale catalogues (2MASS, Skrutskie et al. 2006; UKIRT DR6, Lawrence et al. 2007; DENIS, Epchtein et al. 1994). Table 4 lists the magnitudes available from these sources, where the magnitudes were transformed into those in the IRSF photometric system (Kato et al. 2007). The magnitudes in the DENIS and UKIRT DR6 photometric systems were transformed into the 2MASS system by using the equations in Carpenter (2001) and Hewett et al. (2006), respectively, and then further transformed into the IRSF system by using Kato et al. (2007). The J, H, and $K_{\rm s}$ magnitudes list in Table 4 and show significant variations. The mean magnitudes are obtained by taking averages of four or three independent data in Table 4.

Here we check the uncertainty in the transformation between the different catalogs by comparing the magnitudes of stars around our Miras after the transformation into the IRSF magnitude. The infrared magnitudes well match between the 2MASS, UKIRT, and IRSF photometry measurements within their uncertainties, whereas the $K_{\rm s}$ magnitudes obtained from the DENIS are different from those in the others by ~ 0.3. We added a shift to the above DENIS magnitudes to fit them onto the 2MASS magnitude scale (the magnitudes in Table 4 are on this corrected scale).

We estimate the uncertainties in the random-phased mean magnitudes in the $K_{\rm s}$-band as follows. Carbon-rich Miras with periods of 300−350 days in the solar neighborhood and nearby dwarf galaxies appear to have $K_{\rm s}$-band amplitudes of 0.5–1.0 mag (Whitelock

et al. 2003). O-rich Miras with periods of 100−150 days have the $K_{\rm s}$-band amplitude of 0.14−0.88 mag in the sample of Whitelock et al. (2000). The amplitudes of #1 and #2 are assumed to be 0.75 mag and 0.51 mag in the K_s-band, respectively, suggesting that the observed mean magnitudes are located within ± 0.38 mag and ± 0.26 mag around their true mean magnitudes, respectively. Our infrared datasets consist of four and three independent data for #1 and #2, and thus the uncertainties in the mean magnitudes are approximately 0.19 mag and 0.15 mag.

2.4. Distances and radial velocities

To discuss whether or not our target stars are associated with the Sextans dSph, we estimate the distances on the basis of the period-luminosity (PL) relation of Miras. Miras, as well as semi-regulars with a relatively regular variation and an amplitude close to 1 mag, like #2, are generally found to lie on the Mira PL relation. Thus, we can apply this relation to both of our targets (Ita et al. 2004ab).

Adopting the distance modulus of the LMC to be 18.50 ± 0.02 (Alves 2004), the PL relation for the Miras (Ita & Matsunaga 2011) is expressed as

$$M_K = (-3.675 \pm 0.076) \log P + (1.456 \pm 0.173). \quad (2)$$

Ita & Matsunaga (2011) also found that the redder Miras tend to show large offsets from the PL relation. They suggested that such offsets are caused by the dust shells around red Miras ($J - K_{\rm s} \gtrsim 2$), and we discuss the implication for our Miras in Section 3. For #1, the offset in the $K_{\rm s}$ band is estimated to be 0.12 ± 0.09 mag (Ita & Matsunaga 2011). In contrast, the target #2 is so blue that such an offset is negligible, if any. The interstellar extinctions in the Galaxy in the $K_{\rm s}$ band are calculated to be 0.02 mag from the map in Schlegel et al. (1998).

After correcting the above offset and the interstellar extinction, we obtain distances of $75.3^{+12.8}_{-10.9}$ kpc and $79.8^{+11.5}_{-9.9}$ kpc for the targets #1 and #2. The uncertainties in the distances include those in periods, period-luminosity relation, and mean $K_{\rm s}$-band magnitudes. The estimated distances are consistent with that of the Sextans dSph, 90.0 ± 10.0 kpc (Lee et al. 2003, 2009).

Here we discuss the effect of the long-term trend on the distance esitmate for #1. Long-term trends have been detected from optical and infrared wavelengths, however the relationship among different wavelengths has not been established, in particular when our data points are poor. In addition, the observation dates for the 2MASS and the UKIRT were MJD 51174 and 53726, respectively, whereas our I_c observations started on MJD=54836. The long interval between the infrared and the I_c observations makes the estimation of the long-term trend difficult. However, the long-term trend is suggested to be partly related with absorption by the circumstellar dust (Winters et al. 1994). The circumstellar extinction is also suggested to be correlated with the deviation from the PL relation (Ita & Matsunaga 2011), and its deviation is corrected using the $(H - K_{\rm s})$ color in this work. Thus, the above correction considering the $(H - K_{\rm s})$ color works, at least partly, as the correction of the long-term trend. In fact, the UKIRT photometry indicates that the #1 was both fainter and redder at its epoch than at the epochs of other photometry. Even if we exclude the UKIRT magnitudes from our calculation, with the proper correction applied, we get the same result within the uncertainty.

We check the reliablity of the distance for #2. The Ic-band PL relation in Ita & Matsunaga (2011) is relatively tight near the period of our Mira #2 (P=122 days), although it has a higher dispersion than the Ks-band PL relation. The distance based on the Ic-band PL relation is estimated to be $86.6^{+23.1}_{-18.2}$ kpc, consistent with the distance by the Ks-band PL relation ($79.8^{+11.5}_{-9.9}$ kpc).

The systematic radial velocity of the Sextans dSph is 226.0 km s^{-1} with a dispersion of 8.4 km s^{-1} (Battaglia et al. 2011). For the targets #1 and #2, the radial velocities at a single epoch are 202 ± 12 km s^{-1} (Mauron et al. 2004) and 228.2 ± 2 km s^{-1} (Suntzeff et al. 1993). The radial velocity of a Mira measured with the optical spectra shows a time variation due to the pulsation by 10–25 km s^{-1} (Alvarez et al. 2001). The radial velocities of foreground stars in the direction of the Sextans dSph show a peak around 0–50 km s^{-1} and a weak tail toward a large velocity. Probabilities of foreground stars with the velocities of our targets are low, and this clearly support the memberships to the Sextans dSph.

Another possible system that the targets might be associated with is a stellar stream in the Galactic halo. The SDSS reveals the presence of a 60-degrees-long stream extending from the Ursa Major to the Sextans (e.g., Grillmair 2006). However, its heliocentric distance is about 20 kpc, much smaller than those of our targets. The model of Law et al. (2005) predicts the presence of the Sagittarius stream at a heliocentric distance of 20-60 kpc toward the Sextans dSph in the oblate dark-matter halo of the Galaxy, although the stream has not been identified in its direction. Furthermore, the predicted radial velocities are 250–290 km s^{-1}, which are larger than the measured values of the targets. Thus, both of our targets are most likely associated with the Sextans dSph.

3. Discussion

As mentioned in Section 1, our targets in the Sextans dSph are expected to be metal-poor. Further constraints can be inferred from their locations in the galaxy. The target #1 is located within the tidal elliptical radius of the Sextans dSph (160 arcmin, ellipticity of 0.35), but in its outer part. Unfortunately, the metallicities for a large sample of stars around the target #1 are not yet available. Nevertheless, Battaglia et al. (2011) reported that the Sextans dSph has a clear metallicity gradient: most stars beyond an

elliptical radius of 48 arcmin (ellipticity 0.35) in projection appear to have [Fe/H]< -2.2, while metal-rich stars are concentrated toward the center. The target #1 is located beyond the elliptical radius of 48 arcmin, suggesting that its metallicity is very low.

As shown in Section 2.4, the target #1 is very red, in particular at the UKIRT epoch, $J - K_{\rm s} = 2.96$. Ita & Matsunaga (2011) suggested the existence of the dust shells around such red Miras from their magnitudes fainter than the PL relation. The deviation of the $K_{\rm s}$ magnitude in each catalog from that of the period-luminosity relation appears to follow a function of the $(J - K_{\rm s})$ and $(H - K_{\rm s})$ in Ita & Matsunaga (2011).Sloan et al. (2009, 2012) and Matsuura et al. (2007) detected the SiC dust excess for the spectra of the carbon-rich AGB stars in nearby metal-poor dSphs. The color and period of target #1 are similar to those in the carbon-rich Miras in Sloan et al. (2012). Thus, we suggest a possible presence of the circumstellar dust around carbon-rich Miras with the metallicity ~ 100 times lower than the solar. The Sextans dSph has a lower mean metallicity than any other dSph in Sloan et al. (2012), and the target #1 can impose an important limit on the metallicity dependence of the dust content around carbon-rich Miras.

The target #2 is located in the inner part of the Sextans dSph. In contrast to the outer part, relatively metal-rich stars ([Fe/H]> -1.0) coexist with the metal-poor stars at the inner part, and thus the limit on the metallicity of #2 is not so strong. The short-period and oxygen-rich chemistry suggest that the target #2 is similar to low-mass Miras found in Galactic globular clusters.

4. Summary

We discovered two Miras ($P = 326$ and 122 days, respectively) toward the metal-poor Sextans dSph by performing photometric monitoring for red stars over periods of 3-4

years, although the shorter-period one may be a semi-regular. The distances and radial velocities of the objects are consistent with those of the Sextans dSph, which suggests that the two objects belong to the Sextans dSph. Thus, these objects are found in the lowest metallicity dSph with Miras, [Fe/H]< -2. The red near-infrared color of the longer-period Mira #1 suggests the presence of circumstellar dust in a system with the lowest metallicity. Follow-up spectroscopic observations in the infrared wavelengths is useful to investigate dust formation in the very metal-poor objects.

We thank Aoki, T., Soyano, T., Tarusawa, K., and Dr. Mito, H. for supporting our observations at Kiso observatory. We are grateful to Dr. Feast, M. W. for reading the manuscript carefully and for his comments. TS thanks Dr. Ita, Y. for providing the source code of the period determination. NM acknowledges the support of Grant-in-Aid for Young Scientists (No 23684005) from the Japan Society for the Promotion of Science (JSPS). Funding for the SDSS and SDSS-II has been provided by the Alfred P. Sloan Foundation, the Participating Institutions, the National Science Foundation, the U.S. Department of Energy, the National Aeronautics and Space Administration, the Japanese Monbukagakusho, the Max Planck Society, and the Higher Education Funding Council for England. The SDSS Web Site is http://www.sdss.org/.

REFERENCES

Adelman-McCarthy J. et al. 2008, ApJS, 175, 297

Alvarez, R., Jorissen, A., Gillet, D., Fokin, A., & Dedecker, M. 2001, A&A, 379, 305

Alves D. R. 2004, New Astronomy Reviews, 48, 659

Battaglia, G., Tolstoy, E., Helmi, A., Irwin, M., Parisi, P., Hill, V., & Jablonka, P. 2011, MNRAS, 411, 1013

Carpenter 2001, AJ, 121, 2851

Cruz K. L., Reid, I. N., Kirkpatrick, J. B., et al. 2007, AJ, 133, 439

Epchtein, N., de Batz, B., Copet, E., et al. 1994, Ap&SS, 217, 3

Feast, M W., Whitelock, P. A., & Menzies, J. W. 2002, MNRAS, 329, L7

Fraser, O. J., Hawley, S. L., & Cook, K. H. 2008, AJ, 136, 1242

Frogel, J. A. & Whitelock, P. A. 1998, AJ, 116, 754

Grillmair, C. J. 2006, ApJ, 645, L37

Groenewegen, M. A. T. 2000, A&A, 363, 901

Groenewegen, M. A. T., Sloan, G. C., Soszyński, I. & Petersen, E. A. 2009, A&A, 506, 1277

Habing, H. J. 1996, A&A Rev., 7, 97

Hewett, P. C., Warren, S. J., Leggett, S. K., & Hodgkin, S. T. 2006, MNRAS, 367, 454

Ita, Y., Tanabe, T., Matsunaga, N., et al. 2004a, MNRAS, 353, 705

Ita, Y., Tanabe, T., Matsunaga, N., et al. 2004b, MNRAS, 353, 705

Ita, Y. & Matsunaga, N. 2011, MNRAS, 412, 2345

Itoh, N., Soyano, T., Tarusawa, K., Aoki, T., Yoshida, S., Hasegawa, T., Yadomaru, Y., Nakada, Y., & Miyazaki, S. 2001, Publications of the National Astronomical Observatory of Japan, 6, 41

Jordi, K., Grebel, E. K., & Ammon, K. 2006, A&A, 460, 339

Kato, D., Nagashima, C., Nagayama, T., et al. 2007, PASJ, 59, 615

Kirby, E. N., Guhathakurta, P. Bolte, M., Sneden, C., & Ghea, M. C. 2009, ApJ, 705, 328

Lagadec, E., Zijlstra, A. A., Sloan, G. C., et al. 2009, MNRAS, 396, 598

Lawrence, A., Warren, S. J., Almaini, O., et al. 2007, MNRAS, 379, 1599

Law, D. R., Johnston, K. V., & Majewski, S. R. 2005, ApJ, 619, 807

Lee, M. G., Park, H. S., Park, J., et al. 2003, AJ, 126, 2840

Lee, M. G., Yuk, I., Park, H. S., Harris, J., & Zaritsky, D. 2009, ApJ, 703, 692

Mateo, M. Fischer, P. & Krzeminski, W. 1995, AJ, 110, 2166

Matsunaga, M., Fukushi, H., & Nakada Y. 2005, MNRAS, 364, 117

Matsuura, M., Zijlstra, A. A., Bernard-Salas, J., et al. 2007, MNRAS, 382, 1889

Matsuura, M., Barlow, M. J., Zijlstra, A. A., et al. 2009, MNRAS, 396, 918

Mauron, N., Azzopardi, M., Gigoyan, K., & Kendall, T. R. 2004, A&A, 418, 77

Menzies, J. W., Whitelock, P. A., Feast, M. W., & Matsunaga, N. 2010, MNRAS, 406, 86

Menzies, J. W., Feast, M. W., Whitelock, P. A., & Matsunaga, N. 2011, MNRAS, 414, 3492

Nagayama, T. et al. 2003, Proc. SPIE, 4841, 459

Norris, J. E., Wyse, R. F. G, Gilmore, G., Yong, D., Frebel, A., Wilkinson, M. I., Belokurov, V., & Zucker, D. B. 2010, ApJ, 723, 1632

Rengstorf, A. W., Thompson, D. L., Mufson, S. L., et al. 2009, ApJS, 181, 129

Schlegel, D. J., Finkbeiner, D. P., & Davis, M. 1998, ApJ, 500, 525

Skrutskie, M. F., Cutri, R. M., Stiening, R., et al. 2006, AJ, 131, 1163

Sloan, G. C., Matsuura, M., Zijlstra, A. A., Lagadec, E., Groenewegen, M. A. T., Wood, P. R., Szyszka, C., Bernard-Salas, J., & van Loon, J. Th. 2009, Science, 323, 353

Sloan, G. C., Matsuura, M., Lagadec, E., et al. 2012, astroph/1204.5754

Soszyński, I., Udalsky, A., Szymañski, M. K, et al. 2009, Acta Astron., 59, 239

Stellingwerf, B. F. 1978, ApJ, 224, 953

Suntzeff, N. B., Mateo, M., Terndrup, D. M., Olszewski, E. W., Geisler, D., & Weller, W. 1993, ApJ, 418, 208

Whitelock, P. A., Marang, F., & Feast, M. W. 2000, MNRAS, 319, 728

Whitelock, P. A., Feast, M. W., van Loon, J. Th. & Zijlstra, A. A. 2003, MNRAS, 342, 86

Whitelock, P. A. Menzies, J. W., Feast, M. W., Matsunaga, N., Tanabe, T., & Ita, Y. 2009, MNRAS, 394, 795

Winters, J. M., Fleischer, A. J., Gauger, A., Sedlmayr, E. 1994, A&A, 290, 623

Fig. 1.— (Top): I_c-band light curves of our targets. The arrows indicate the epochs of the IRSF near-infrared data. (Bottom): Phased light curves. For #1 the long-term trend is substracted.

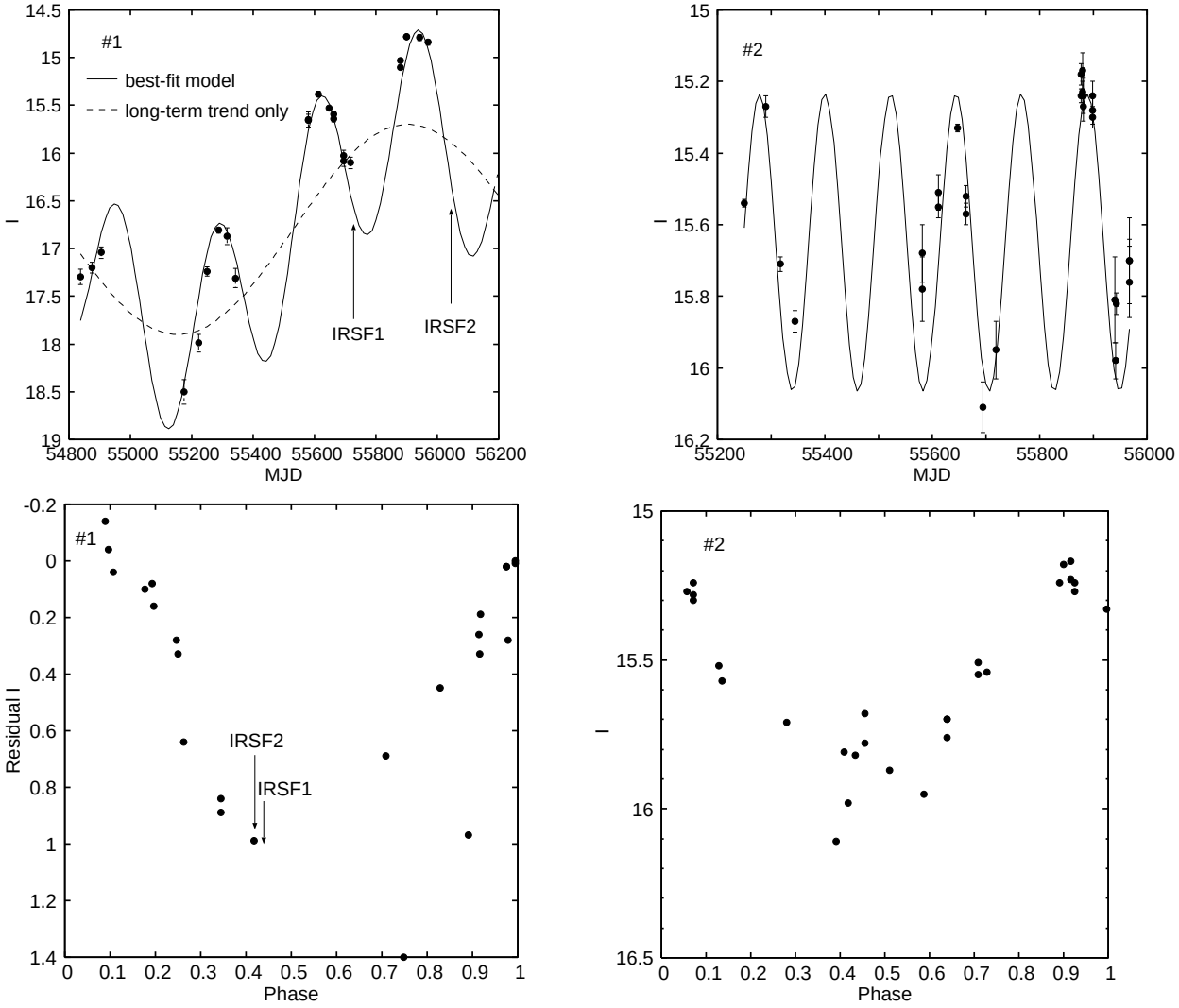

Table 1. List of our target stars. The magnitudes $< I_c >$ denote the mean magnitude of the targets in the I_c-band, whereas ΔI_c show their amplitudes. The distances obtained by us are listed as well as the radial velocities and the chemistry types.

ID	RA (J2000)	DEC (J2000)	Period (days)	$< I_c >$ (mag)	ΔI_c (mag)	Distance (kpc)	Radial velocity (km s^{-1})	Carbon-rich/ Oxygen-rich
#1 (SDSS J101525.93−020431.8)	10:15:25.93	−02:04:31.8	326 ± 15	17.0	3.72	$75.3^{+12.8}_{-10.9}$	202 ± 12[c]	Carbon-rich[c d]
#2 (SDSS J101234.29−013440.8)	10:12:34.29	−01:34:40.8	122 ± 5	15.7	0.94	$79.8^{+11.5}_{-9.9}$	228.2 ± 2.0[e]	Oxygen-rich[e]
Sextans dSph	10:13:03	−01:36.9	—	—	—	$90.0^{+10.0a}_{-10.0}$	226 ± 8.4[b]	—

[a]Average of Lee et al. (2003) and Lee et al. (2009)

[b]Battaglia et al. (2011)

[c]Mauron et al. (2004)

[d]Cruz et al. (2007)

[e]Suntzeff et al. (1993)

Table 2: Time-series photometric results for our target #1. Modified Julian Date (MJD), the I_c-band magnitude, and the photometric error is listed for each image we took.

#1 (SDSS J101525.93−020431.8)

MJD	I_c (mag)	e_{I_c} (mag)	MJD	I_c (mag)	e_{I_c} (mag)
54836.77	17.30	0.08	55646.49	15.53	0.01
54875.69	17.20	0.06	55662.53	15.59	0.02
54904.57	17.04	0.06	55663.49	15.64	0.03
55174.78	18.50	0.13	55694.50	16.08	0.06
55221.64	17.99	0.09	55694.50	16.03	0.06
55249.61	17.24	0.05	55718.48	16.10	0.06
55288.48	16.81	0.03	55879.84	15.03	0.02
55314.58	16.87	0.09	55880.82	15.10	0.02
55342.49	17.31	0.10	55899.85	14.78	0.01
55580.79	15.66	0.07	55899.85	14.78	0.02
55580.79	15.65	0.08	55942.73	14.79	0.03
55611.56	15.38	0.03	55970.55	14.84	0.03

Table 3: Same as Table 2, but the target #2.

#2 (SDSS J101234.29−013440.8)								
MJD	I_c (mag)	e_{I_c} (mag)	MJD	I_c (mag)	e_{I_c} (mag)	MJD	I_c (mag)	e_{I_c} (mag)
55249.60	15.54	0.01	55663.49	15.57	0.03	55898.73	15.24	0.04
55289.42	15.27	0.03	55694.50	16.11	0.07	55898.73	15.30	0.03
55316.47	15.71	0.02	55718.47	15.95	0.08	55939.77	15.81	0.12
55344.47	15.87	0.03	55876.77	15.24	0.02	55940.76	15.98	0.05
55580.78	15.68	0.08	55877.78	15.18	0.03	55942.72	15.82	0.03
55580.78	15.78	0.09	55879.83	15.17	0.05	55967.70	15.70	0.12
55611.55	15.55	0.03	55879.84	15.23	0.03	55967.70	15.76	0.10
55611.55	15.51	0.05	55880.81	15.24	0.05	55967.70	15.70	0.06
55646.65	15.33	0.01	55880.81	15.27	0.04			
55662.53	15.52	0.03	55898.72	15.28	0.04			

Table 4: J, H, and K_s magnitudes of our targets available in our photometry with the IRSF/SIRIUS and other near-infrared catalogs.The magnitudes in other photometric systems were transformed into the IRSF system.

Object		#1				#2		
Filter	MJD	J	H	K_s	MJD	J	H	K_s
2MASS	51174.35	14.017 ± 0.026	12.908 ± 0.025	11.981 ± 0.026	51174.31	14.128 ± 0.022	13.567 ± 0.029	13.391 ± 0.036
UKIRT	53726.68	15.142 ± 0.005	13.596 ± 0.004	12.179 ± 0.004	53726.68	13.853 ± 0.002	13.303 ± 0.002	13.139 ± 0.003
IRSF1	55726.76	13.830 ± 0.005	12.470 ± 0.005	11.430 ± 0.005	—	—	—	—
IRSF2	56045.76	13.420 ± 0.005	12.470 ± 0.005	11.430 ± 0.005	—	—	—	—
DENIS	—	—	—	—	50480.25	—	—	13.34 ± 0.17
Average	—	14.10	12.86	11.76	—	13.99	13.43	13.34